Korean J. Chem. Eng., **30**(2), 262-268 (2013)
DOI: 10.1007/s11814-012-0211-0

REVIEW PAPER

The solids concentration distribution in the deep cone thickener: A pilot scale test

Huazhe Jiao*·, Aixiang Wu**, Hongjiang Wang**·†, Shuiping Zhong*, Renman Ruan*, and ShengHua Yin****

*State Key Laboratory of Comprehensive Utilization of Low-Grade Refractory Gold Ores, Zijin Mining Group Co., Ltd., Shanghang 364200, China
**School of Civil and Environment Engineering, University of Science and Technology Beijing, Beijing 100083, China
(*Received 1 February 2012 • accepted 6 December 2012*)

Abstract−Cemented backfill or surface deposition of paste tailings is increasingly being considered as a simple and effective means of reducing the hazards of conventional slurry deposition and recovering water for recycle. Although gravity thickening has been widely used in the mineral industry to increase the solids concentration of tailings, the accurate prediction of the concentration distribution in three-dimensions and discontinuous operational state has proven to be difficult. We investigated the axial and radial solids concentration distribution at discontinuous state in a pilot deep cone thickener as a function of bed height and residence time. The feed flux of lead/zinc tailings was 0.254 $t \cdot h^{-1} \cdot m^{-2}$ with a flocculant (high molecular weight anionic polyacrylamide) dose of 20 g/t. The thickened solids bed was sheared by a rotating rake at a rate of 0.2 rpm. The underflow was recirculated at a flux of 0.5 $t \cdot h^{-1} \cdot m^{-2}$, which can introduce additional shear stresses into the bed. The results of the bed density profile showed that, beside the clarification zone, the area below the feedwell could be divided into four zones: the dilution zone caused by free settling and diffusing action, the hindered settling zone in which the concentration was lower than the gel point, the unraked bed zone with a large concentration gradient and, finally, the raking zone with the highest slurry concentration and lower concentration gradient.

Key words: Thickening, Dewatering, Concentration Distribution, Pilot Scale Deep Cone Thickener

INTRODUCTION

Tailings from mineral processing are waste products that must be disposed to the environment. They can also be very hazardous materials when deposited on the surface, which has caused many deaths around the world in the past century [1,2], such that tailings have been quoted as the No. 6 most hazardous material on the earth [3]. Meanwhile, most of these tailings have been stacked on the surface and there are more than 12,000 tailings ponds in China with over 8 billion tons of metal mine tailings, and this number has increased at a speed of 600 million tons per year [2,4].

Paste backfill or paste surface disposal is an economic and technical way to solve this problem. It has been widely used in Canada, Australia, South Africa, and China.

Gravity thickening, with the advantage of water recycling, is a conceptually simple and effective means of producing high concentration material for backfill and disposal. In the operation, the tailings slurry is fed to a gravity thickener via a feedwell where the flocculant solution is pumped to increase the size of the aggregates. The flocs formed by particles and flocculants settling due to density difference and are discharged as thickened underflow [5].

In the past few decades, theories to predict the performance of continuous thickeners have been reported in the literature [6-11,17]. These models share a common phenomenological basis that dewatering is described by two key compressional rheological functions, a concentration dependent compressive yield stress, $P_y(\phi)$ and a hindered settling function, $R_y(\phi)$.

†To whom correspondence should be addressed.
E-mail: wanghj1988@126.com

The continuous gravitational thickening model, developed by Landman [16] and demonstrated for arrange of materials by Usher and Scales [7], has been applied to several operating thickeners. But there are two problems. First, data comparing of laboratory measurements and model prediction to full scale output are surprisingly scarce, suggesting that this observed shortcoming is widespread [7,15,17]. Second, most of the models were established for continuous steady state operation. However, for the mine backfill operation, some thickeners are designed as both dewatering device and storage tank, which means they cannot discharge continuously.

There is a growing body of evidence showing that shearing a consolidating bed, as in the case in a raked thickener, vastly improves dewaterability. The effect appears to be minor for un-flocculated slurries [18] but is significant when the thickener feed is flocculated. Shearing of flocculated suspensions has been associated with a measured decreased in $R_y(\phi)$ and an increased in the material gel point, ϕ_g [19]. This is postulated to be due to intra-aggregate densification such that $R_y(\phi)$ is lowered and network failure occurs at a lower applied stress for a given volume fraction. This postulate is based on the operational observation that the concentration of thickener output depends on the rotational speed of the rake, type of thickener and cone angle [8,14,15,19]. There is also growing evidence of improvements in $R_y(\phi)$ for systems with an average solids volume fraction less than the gel point [7].

These studies utilized steady state models. However, there would often be intermittent feed and discharges in plant operation, such that the unsteady states would impact the concentration distribution in the thickener.

The test equipment in the published literature has been mostly laboratory scale [7,8,15,20], or discontinuous operation [21,23].

This equipment differs from the full scale, which inevitably has caused deviation between the predictive results and the measured value [13].

The pilot deep cone thickener in this work was multifunctional, with a feedwell, a rake and an underflow circulation pump. The feed slurry and flocculants solution were pumped into the feed well together to ensure the particles were flocculated. Also, the pilot thickener introduced a raking system and underflow circulating system in order to simulate real thickener operation.

The aim of this work was to investigate the concentration distribution in a continuous deep cone thickener by obtaining the transient profiles. In the thickener, the concentrated bed was raked and the underflow was circulated back into the tank. Meanwhile, the underflow volume fraction affected by the bed height and residence time was tested under discontinuous operations. Laboratory scale batch settling experiments [5] were used to establish the inputs for the model to give the expected thickener performance.

EXPERIMENTAL EQUIPMENT, MATERIALS AND METHODS

1. Pilot Scale Deep Cone Thickener

The height of the pilot thickener was 2 m and the diameter was 1.375 m. More details are shown in Fig. 1 and Table 1. Feed is injected in a feedwell at the top of the tank. Overflow is collected by a deposition pool. The schematic of the pilot thickener flow cycle is shown in Fig. 2.

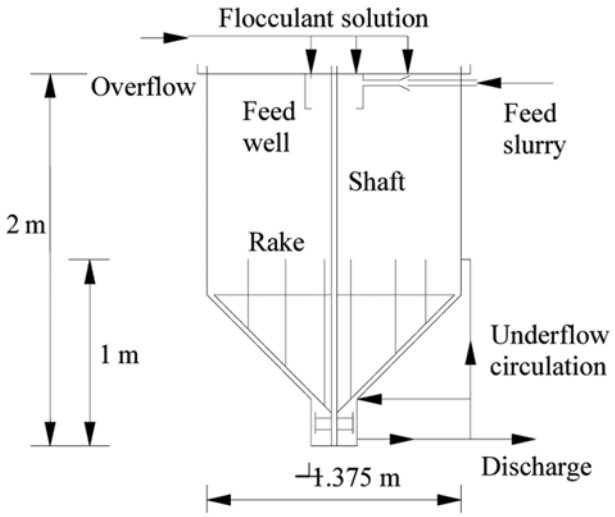

Fig. 1. Pilot scale deep cone thickener.

Table 1. Parameters of the pilot thickener

Diameter (m)	1.375
Height (m)	2
Height of cone (m)	0.8
Angle of cone (°)	45
Volume (m^3)	2.16
Raking speed (rpm)	0.5-1
Circulating flow flux (m^3/h)	0.3-0.7

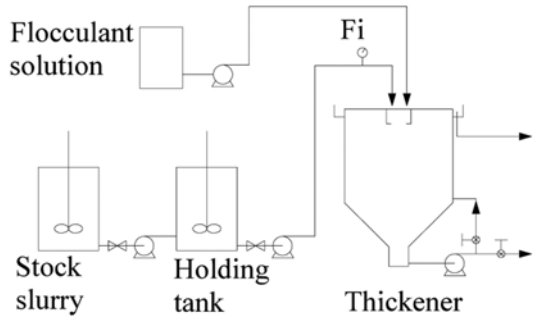

Fig. 2. Pilot Scale Deep cone thickener flow circle.

The pilot thickener can be operated with different raking speeds and underflow circulation fluxes, as shown in Fig. 1.

2. Material

The tailings come from a lead and zinc mine in China with average particle size of 98 μm; the size profile is shown in Fig. 3. The density of the tailings was 2.7 t/m^3, bulk density was 1.85 t/m^3, the porosity was 34.98%.

The gel point was tested in the traditional batch settling method with a rake. The cylinder volume was 1 liter; the rotation speed was

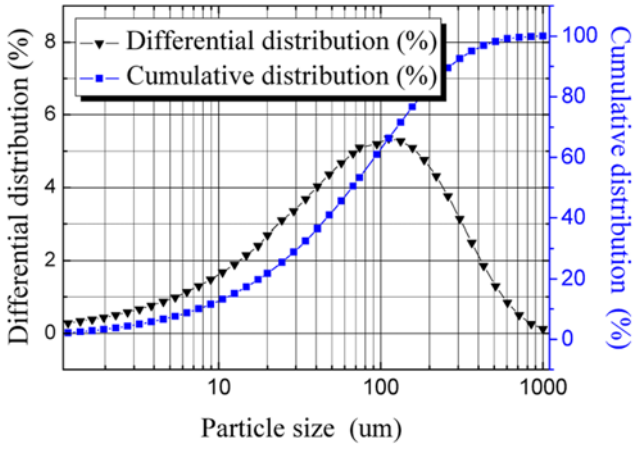

Fig. 3. Particle size distribution of tailings.

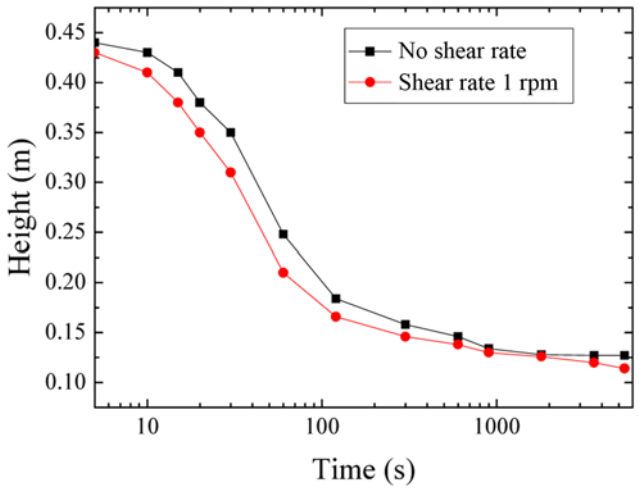

Fig. 4. The batch settling curve.

0.1 rpm (Fig. 4).

With densification of aggregates considered, the gel point was tested according to the test method described by Gladman et al. [24] and van Deventer et al. [25], using the batch cylinder test with a rotating rake.

The results show that with anionic flocculants (PAM) at dosage 20 g/t and at the initial solids concentration 3.5%, the gel point at zero time was about 19.43 v/v%, and the gel point after a constant 900-second shearing was 20.87%.

3. Experimental Methods

3-1. Experimental Control Parameters

A high molecular weight anionic PAM flocculant (AN934SH from SNF), with a dosage of 40 $g \cdot t^{-1}$, was used. The initial polymer solution concentration was 0.1 wt%, which was then diluted to 0.02 wt% when pumped into the tank.

According to the batch settling results [5], the pilot test parameters were determined and are shown in Table 2.

3-2. Sampling Methods

3-2-1. Sampler

To reflect the real concentration distribution, the sampler was immersed and collected with a moveable cover under the water. The sampler is shown in Fig. 5, while the sampling location is shown in Fig. 6.

The sampler was home-made with a long shaft connected to a sample cup with height 10 cm and inner-diameter 5 cm. Movement of the cup was controlled by a connected cover shaft. The sample volume collected each time by this device was calculated as 3.14×0.1 m×0.025 m×0.025 m=196.25 ml, approximately 196 ml.

3-2-2. Sampling Procedure

The samples were collected during bed formation.

The sample collection procedure involved three steps. First, the cup was closed by pushing down the cover shaft, and fixing both shafts together. Second, the sampler was slowly immersed under water to the target position in 1-2 minutes, minimizing the disturbance to the formed bed. Third, the sampler was held steady in position for 20-30 seconds to ensure the minimized disturbance. Fourth, the cover shaft was lifted to open the sample cup for 10 seconds, during which the bed slurry flowed into and filled the cup. Ten seconds later, the cover shaft was pushed back down to close the sample cup and fixed both shafts together. Meanwhile, the cup was held steady in position. Finally, the sampler was slowly raised out of the water.

The volume fraction of the slurry was calculated using Eq. (1) [15].

$$m_t = \frac{\gamma_f - \gamma_0}{\gamma_k - \gamma_0}, \quad (1)$$

γ_0: the density of water, t/m^3;
γ_k: the density of tailings, t/m^3;
γ_f: the density of slurry, t/m^3;
m_t: the volume fraction, %.

The density of slurry was tested by Balloon densimeter whose resolution is 0.01 g/ml. All the slurry samples were tested in the sampler immediately after collection. Consequently, there was no weight loss from sample drying.

Table 2. Experimental parameters

Flocculants dosage (g/t)	40
Flocculants solution concentration (g/t)	0.1
Raking speed (rpm)	0.2
Feeding solids flux ($t \cdot h^{-1} \cdot m^{-2}$)	0.254
Feed solids volume fraction (%)	3.5
Underflow circulation Flux ($t \cdot h^{-1} \cdot m^{-2}$)	0.5
Target thickened bed height ($t \cdot h^{-1} \cdot m^{-2}$)	1.2

(a) Closed (b) Open

Fig. 5. The sampler size and structure.

RESULTS AND DISCUSSION

1. Results

The in situ solids concentration distribution profile was drawn from the sample results, shown in Fig. 6 and Fig. 7.

Three additional values were interpolated between the data points in Fig. 6(a) according to the simulation law [20]. The concentration profiles were formed by testing concentration values. Considering that the thickener tank was of axially symmetric geometry, the concentration contour line inside the thickener was achieved by symmetry, as shown as Fig. 7.

2. Concentration Distribution Analysis

It has long been recognized that the solids in an operational thickener could be divided into several zones, including a clarification, a hindered settling and a thickened bed zone [8,9,15].

As mentioned above, the gel point of this tailing was 19.4-20.9

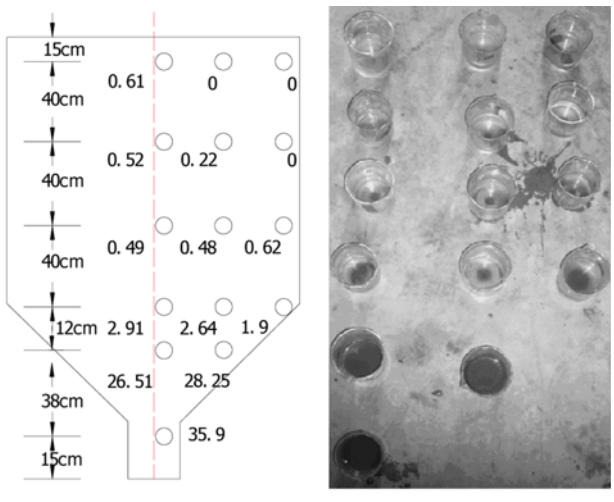

(a) (b)

Fig. 6. Sampling location and concentration results (% v/v).

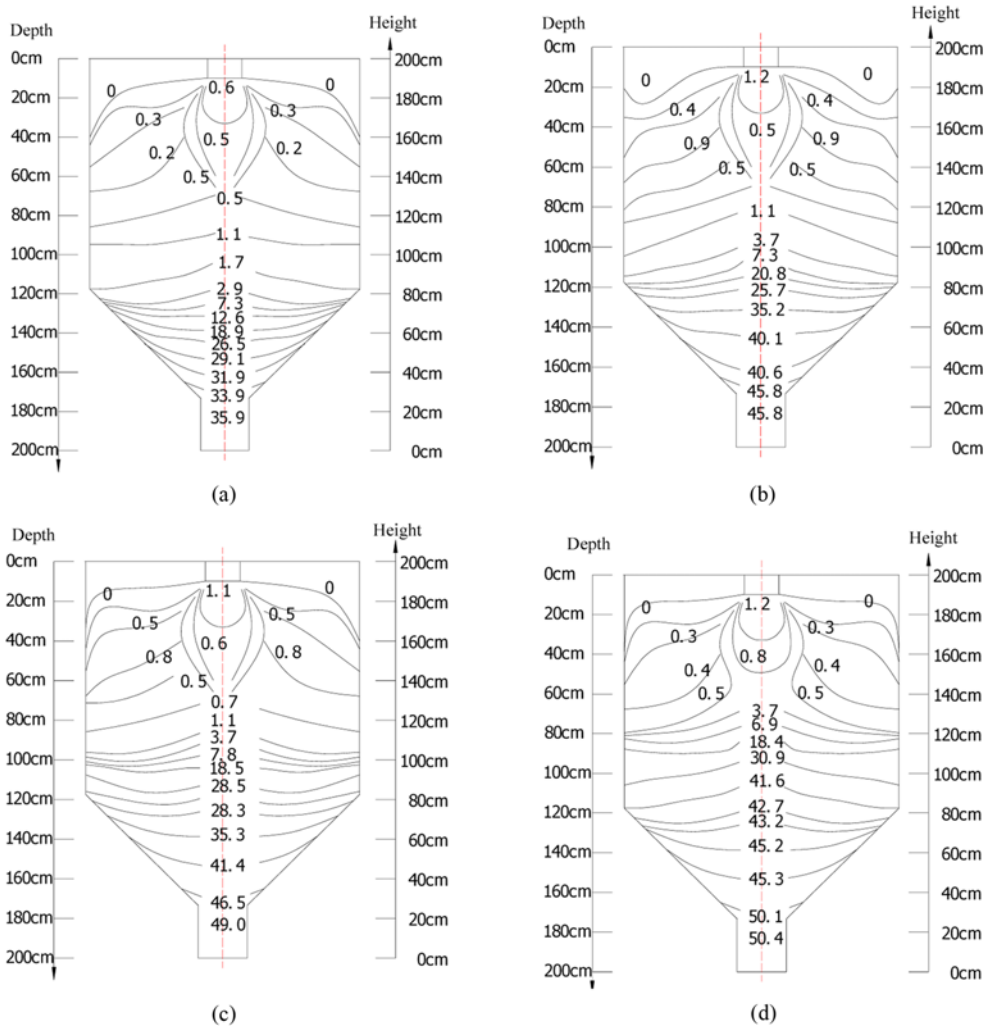

Fig. 7. The inner solids concentration gradient profile in the thickener. Residence time (a) 0.5 h, (b) 1.5 h, (c) 2.5 h, (d) 3.5 h.

v/v% affected by densification. The concentration distribution along the thickener height is shown in Fig. 8.

According to Fig. 8, the bed height increased with the residence time. The corresponding values were 66 cm bed height to 35.9%

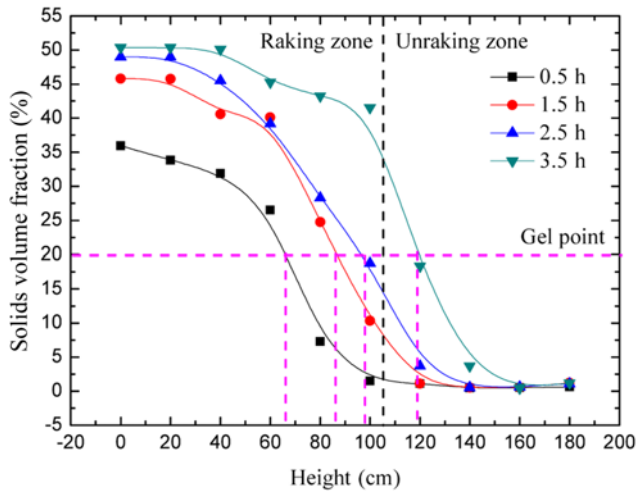

Fig. 8. Solids concentration profile along the height.

at 0.5 h, 87 cm to 45.8% at 1.5 h, 98 cm to 49.0% at 2.5 h and 119 cm to 50.4% at 3.5 h, respectively. The underflow concentration rose with both bed height and residence time.

As shown in Fig. 9, these profiles have similar concentration raising speed characteristics; there were three increasing ranges and a decreased one. Consequently, the concentration profile was divided into five stages. First, there was a clarification zone at the height 185-200 cm, which can be seen clearly in Figs. 6, 7 and 9. Second, there was a dilution zone below the feedwell at height between 130-185 cm. In this area, the concentration was diluted to 0.1-0.8% for the aggregates settling and diffusing. Third, under the dilution zone, the slurry concentration rose slowly to about 5%. Fourth, the volume fraction increased rapidly to 35-45 v/v%. In this period, the gel point separated the bed into two sections with different permeability. The concentration lower than gel point was non-percolating, the higher was percolating. Fifth, the concentration of underflow increased slowly to about 50 v/v%. The area of each stage varied with the bed height and the residence time.

3. Solids Concentration Distribution in the Deep Cone Thickener

As analyzed above, the concentration distribution in deep cone thickener could be divided into five zones, as shown in Fig. 10.

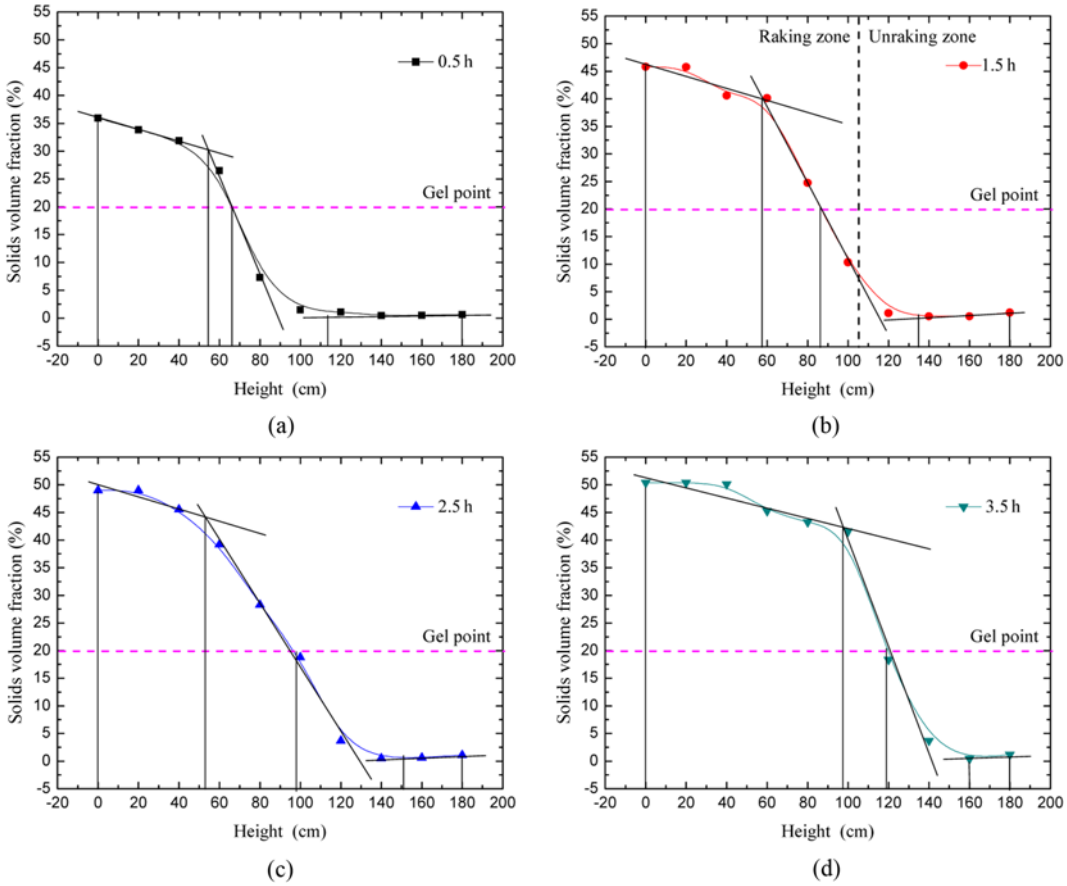

Fig. 9. The profiles of concentration raising velocity.

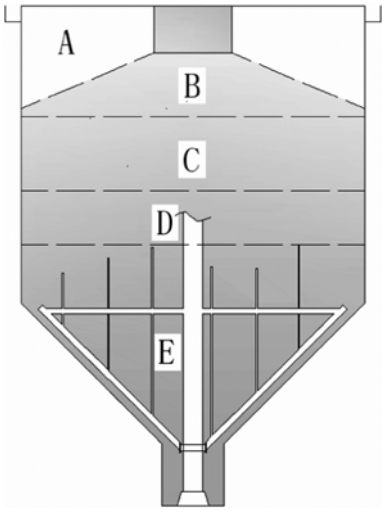

Fig. 10. Concentration zone division in the thickener, A. clarification zone, B. Dilution zone, C. Hindered settling zone, D. Un-raked bed zone, E. Raking zone.

These zones were discussed as follows.

3-1. Clarification Zone

As shown in Fig. 11, the overflow was very limpid. The angle of the clarification zone surface versus horizontal surface was about 5-10°.

After settling out of the feedwell, the aggregates radiated circularly along with the liquid stream. Particles in the stream were impacted by four forces: vertical buoyancy, drag force of horizontal flow, drag force of updraft flow and gravity. The stress analysis is shown in Fig. 12.

Fig. 11. The products of thickener. (a) Underflow, (b) Overflow.

In Fig. 12, F_a is drag force of vertical flow, F_b is buoyancy, F_s is drag force of horizontal flow, G is the gravity, G′ is the downward composite force, G′ could be obtained from Eq. (2).

$$G' = G - F_b - F_a \tag{2}$$

The subscript α denotes the angle of composite force, which is calculated using

$$\tan\alpha = \frac{G'}{F_s}. \tag{3}$$

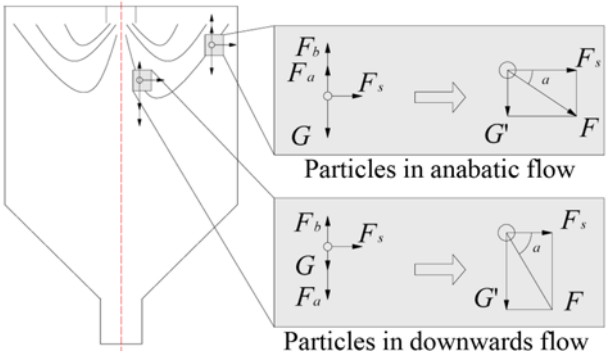

Fig. 12. The force analysis of tailing aggregates.

F is obtained using,

$$F=G'/\sin\alpha. \quad (4)$$

F is the composite force on the particle, which causes the clarification area trapezoid (see Fig. 15).The clarification shape depends on the angle of the shape trapezoid.

3-2. Dilution Zone

As shown in Fig. 6, the cross section became several times large when feed flowed out of the feedwell, so that the local concentration decreased from 3.5% initial fraction to less than 1%. This zone was located below the feedwell at the height 130-185 cm.

3-3. Hindered Settling Zone

This zone has been termed a hindered settling zone by many authors. Coe and Clevenger [21] proposed that the settling rate was a function of solids concentration as long as no mechanical support was contributed from layers of suspension below [15,16].

They called this condition free settling. Indeed, using the theory of Landman and White [18], the free settling rate, $u_{fs}(\phi)$, of a suspension in the absence of a compressive yield stress influence is predicted to be a function of the solids volume fraction, ϕ, according to the following:

$$u_{fs}(\phi) = \frac{\Delta\rho g(1-\phi)^2}{R(\phi)} \quad (5)$$

3-4. Un-raked Bed Zone

Below the hindered settling zone, there is often a networked bed, with a solids concentration greater than the gel point, where the shear and compressive yield stress synergize. Because of the rotating rakes, the concentration of the sheared bed easily reaches 35-45%, as shown in Fig. 8.

There was an settlement interface, that was the boundary between the un-networked and networked zones in a thickener.

In this region, the residence time of the solids in the suspension bed is long enough for compressive dewatering. As such, the amount of compressive force transmitted by the network structure within the bed was the dominant factor that governed the solids fraction.

The solids concentration gradient in this zone was steep as shown in Fig. 9. The material density decreases dramatically from 40% to 20% within a small bed height. As such, this portion of slurry in a thickener could not be discharged for paste backfill.

3-5. Raking Zone

Thickener modeling by Usher [26] predicted gravity thickener performance. For a given solids flux, the underflow solids concentration increased along with the bed height to a upper bound, after which the performance was permeability limited.

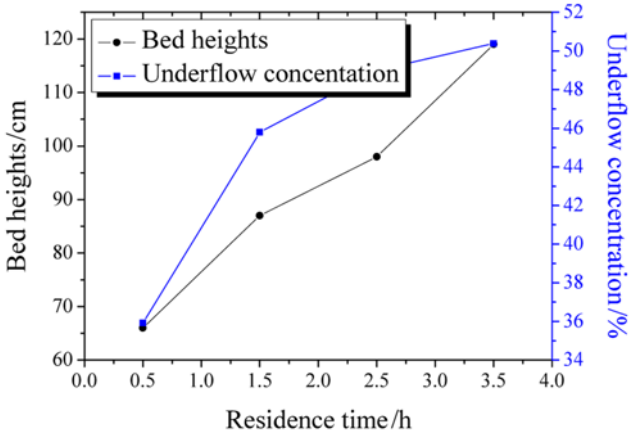

Fig. 13. Underflow concentration in continuous feed.

In this stage, we propose that the dominant effect is the residence time rather than bed height. The analysis is in the following section.

4. The Underflow Concentration

4-1. The Influence of Bed Height

In continuous operation, the bed height increased from 65 cm to 120 cm with residence time, and the underflow concentration rose from 35% to 50% (see Fig. 13).

Greater bed height corresponds to larger self weight, which renders the shear force large enough to overcome the compressive yield stress. If the compressive force is increased through making the higher bed height, the residence time will increase as well.

The compressibility of the material is crucial; choosing conditions to minimize the compressive yield stress would maximize the solids volume fraction of the underflow.

4-2. The Influence of Residence Time

The feed was stopped when residence time (operation time) exceeded 3.5 h, when the bed was so high as to reach the feedwell (Fig. 7(d)). The thickener operated discontinuously. As shown in Fig. 13, the bed surface height declined at a speed of 5 cm/h from

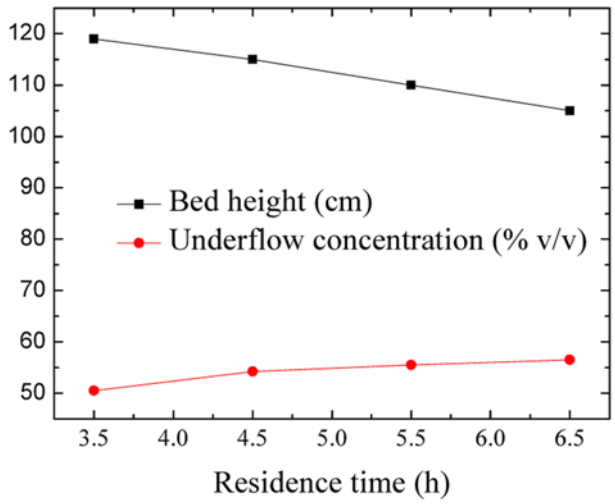

Fig. 14. The underflow concentration in non-continuous operation.

120 cm to 105 cm in the following 3 hours. Meanwhile, the underflow concentration increased from 50.5% to 56.5% (Fig. 14). In conclusion, the solid underflow exhibited a significant dependence on both residence time and the shear rate contributed by the unnetworked bed.

Usher and Scales (2005) [26] have established the calculation methods of the solids residence time in the steady state, as Eq. (6).

$$t_{res} = \frac{1}{q}\int_0^{h_b} \beta(z)\phi(z)dz. \quad (6)$$

Where, q is the solids flux; h_b is the bed height; $\phi(z)$ is the solids concentration at the height of z; $\beta(z)$ is the thickener shape factor, defined as,

$$\beta(z) = \left(\frac{d(z)}{d_{max}}\right)^2, \quad (7)$$

accounts for the cross section area variations with height in the thickener, z. The definition of $\beta(z)$ is such that β=1 when the thickener diameter, d(z), is at its maximum, d_{max}, and the cross sectional area is also maximized.

But, in industry utilization, steady state has always been associated with continuous operation such as the procedure of mineral processing and water treatment operation. Thickeners under steady state are characterized by a constant continuous feed flux, constant bed height and a constant continuous discharge flux.

For the backfilling system in a mine, the thickeners run under discontinuous state. Pauses occur when no goaf needed to be filled, or the thickener capacity was superfluous. Furthermore, accidents such as backfilling pipeline block off also stop the discharging.

One important attention of this paper was focused on the non-discharging stage of discontinuous thickener operation. The residence time was calculated from the moment the solids are being pumped into the thickener feedwell [24,7].

The other way to get the higher solids concentration is to decrease the solids flux, which can also achieve longer residence times and higher bed heights.

CONCLUSION

The solids concentration distribution test was conducted in a discontinuous pilot thickener. The concentration profile can be divided into five sections by density gradient: clarification zone, dilution zone, hindered settling zone, un-raked bed zone, raking zone.

Established literature assumed that boundary surface between clarification zone and solids zones was horizontal. However, the aggregates stress analysis in this paper shows that the boundary surface has an angle which is determined by feed flux, settlement velocity, and feedwell efficiency. Meanwhile, the concentration profile and concentration raising velocity profile show that there is a dilution zone under the feedwell. In addition, the thickened bed, with solids fraction higher than the gel point, can be divided into the unraked bed zone and raking zone based on the large discrepancy of concentration gradient.

Further work should focus on developing more complex functions which include effects such as the impact of unsteady underflow discharge on densification speed, the underflow circulation flux on the concentration gradient.

ACKNOWLEDGEMENTS

This project was supported by the Open Foundation of the State Key Laboratory of Comprehensive Utilization of Low-Grade Refractory Gold Ores, the National Natural Science Foundation of China Key Program (50934002), the Program for Changjiang Scholars and Innovative Research Team in University (IRT0950), and the National Natural Science Foundation of China (51074013, 51104011).

REFERENCES

1. D. Z. Zhang, *China Mine Engineering*, **39**(2), 49 (2010).
2. A. X. Wu, *Granular dynamic theory and its applications*, Metallurgical Industry Press & Springer (2008).
3. R. G. Kretser, P. J. Scales and D. V. Boger, *British Society of Rheology*, **12**, 125 (2003).
4. X. H. Liu, A. X. Wu and H. J. Wang, *Metal Mine*, **9**, 38 (2009).
5. H. Z. Jiao, H. J. Wang and A. X. Wu, *Journal of University of Science and Technology Beijing*, **6**, 702 (2010).
6. Y. G. Zhai, A. X. Wu and H. J. Wang, *Journal of University of Science and Technology Beijing*, **7**, 629 (2011).
7. S. P. Usher, R. Spehar and P. J. Scales, *Chem. Eng. J.*, **151**, 202 (2009).
8. R. Bürger, K. H. Karlsen and J. Towers, *Chem. Eng. J.*, **111**, 119 (2005).
9. P. Mpofu, J. A. Mensah and J. Ralston, *J. Colloid Interface Sci.*, **271**, 145 (2004).
10. M. S. Zbik, R. Smart and G. E. Morris, *J. Colloid Interface Sci.*, **328**, 73 (2008).
11. B. Braggs, D. Fornasiero and J. Ralston, *Clays Clay Minerals*, **2**, 123 (1994).
12. E. Tombaz and M. Szekeres, *Appl. Clay Sci.*, **34**, 105 (2006).
13. J. H. Du, R. A. Pushkarova and R. St. C. Smart, *Int. J. Miner. Process*, **93**, 66 (2009).
14. P. T. Shannon, R. D. Dehaas and E. P. Stroupe, *Ind. Eng. Chem. Fundamentals*, **3**, 250 (1964).
15. E. M. Tory and P. T. Shannon, *Ind. Eng. Chem. Fundamentals*, **4**, 194 (1965).
16. K. A. Landman, L. R. White and R. Buscall, *AIChE J.*, **34**, 239 (1988).
17. S. P. Usher, *Suspension dewatering characterization and optimization*, P.h. D. Thesis, The University of Melbourne, Australia (2002).
18. K. A. Landman, L. R. White and M. Eberl, *Adv. Colloid Interface Sci.*, **51**, 175 (1994).
19. B. Gladman, R. G. Kretser and M. Rudman, *Chem. Eng. Res. Design*, **83**, 1 (2005).
20. R. Bürger, S. Evje and K. H. Karlsen, *Chem. Eng. J.*, **80**, 91 (2000).
21. H. S. Coe and G. H. Clevenger, *Trans. AIME*, **55**, 356 (1916).
22. W. Wang and J. P. Tan, *Mining and Metallurgical Engineering*, **1**, 44 (2004).
23. R. Buscall and L. R. White, *J. Chem. Soc., Faraday Trans.*, **83**, 873 (1987).
24. B. R. Gladman, M. Rudman and P. J. Scales, *Chem. Eng. Sci.*, **65**, 13 (2010).
25. B. B. G. van Deventer, S. P. Usher, A. Kumar, M. Rudman and P. J. Scales, *Chem. Eng. J.*, **171**, 141 (2011).
26. S. P. Usher and P. J. Scales, *Chem. Eng. J.*, **111**(2-3), 253 (2005).